Inorganic Chemistry

Article

pubs.acs.org/IC

Effect of D-Amino Acid Substitutions on Ni(II)-Assisted Peptide Bond Hydrolysis

Hanieh H. Ariani, Agnieszka Polkowska-Nowakowska, and Wojciech Bal*

Institute of Biochemistry and Biophysics, Polish Academy of Sciences, Pawinskiego 5a, 02-106 Warsaw, Poland

Supporting Information

ABSTRACT: Previously we demonstrated the sequence-specific hydrolysis of the R_1-(Ser/Thr)-peptide bond in Ni(II) complexes of peptides with a general R_1-(Ser/Thr)-Xaa-His-Zaa-R_2 sequence (R_1 and R_2 being any sequences) (Kopera, E.; Krezel, A.; Protas, A. M.; Belczyk, A.; Bonna, A.; Wyslouch-Cieszynska, A.; Poznanski, J.; Bal, W. *Inorg. Chem.* **2010**, *49*, 6636). In order to refine our understanding of the mechanism of this reaction and to find ways to accelerate it, we undertook a systematic study of effects of D-amino acid substitutions in the template Ac-Gly-Ala-Ser-Arg-His-Trp-Lys-Phe-Leu-NH_2 peptide on the hydrolysis rate constants. We found that all stereochemical alterations made around the Ni(II) chelate plane resulted in the decrease of the reaction rate. However, the Ni(II) coordination, a prerequisite to the reaction, was not compromised by these substitutions. We demonstrated that the reaction is only possible when either the side chain of the crucial Ser (or Thr) residue is on the same part of the chelate plane as the next residue in the sequence (Arg), or the side chain of the residue following His (Trp) resides on the opposite side of the plane. The rate of reaction is the fastest when both these conditions are fulfilled. Another novel effect is the strong dependence of the rate of the acyl shift step on the character of the leaving group.

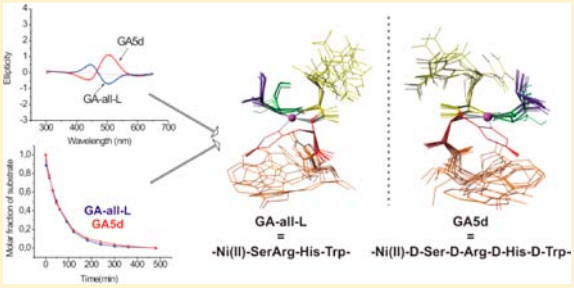

INTRODUCTION

Biological chemistry of nickel(II) is a target of wide investigations due to known toxicity and carcinogenicity of this ion in humans.[1,2] Among the proposed molecular mechanisms of nickel carcinogenesis, we, as well as others, considered histones, the most abundant proteins in eukaryotic cell nuclei,[3] as suitable targets for Ni(II) binding and reactivity.[4−11] In the course of these studies, we found out that the interaction of Ni(II) with the C-terminal tail of histone H2A resulted in sequence-specific hydrolysis of a single peptide bond, both *in vitro* and *in vivo*.[7,8,12] Using oligopeptide library screening and in-depth studies of reactivity of individual peptides, we succeeded in establishing the general mechanism of this reaction. It requires a R_1-(Ser/Thr)-Xaa-His-Zaa-R_2 sequence (R_1 and R_2 being any peptides) and is selective to the peptide bond preceding the Ser/Thr residue. The reaction consists of three essential steps (Scheme 1).[13,14] The first step includes the formation of a square-planar complex anchored at a His residue side chain, involving three preceding amide nitrogens. The last of these nitrogens belongs to a Ser or Thr residue. This enables an acyl shift of this nitrogen toward the alcoholic oxygen in the side chain, which yields an ester intermediate product. The ester then undergoes spontaneous hydrolysis by water, completing the peptide bond cleavage. Our previous studies also showed that the bulky amino acids in Z and X positions accelerated the reaction very significantly, complementing the mechanism of hydrolysis, which thus relies on the molecular crowding in the neighborhood of the hydrolyzed peptide bond. Our recent study of zinc finger peptide hydrolysis demonstrated, however, that sequences which were ranked as inactive in library studies may become activated, when part of longer peptides.[15] This fact urged us to perform a further study of sterical requirements of the reaction.

The peptides used in the present study stem from the pattern used in previous research.[13,14] The model peptide Ac-GA-SRHWKFL-NH_2 was previously selected as the most susceptible to hydrolysis in the presence of Ni(II) ions. We used it as a template, in which we made specific modifications with D-amino acids, in order to study effects of side chain orientations unexplored previously.

Another potential merit of the usage of D-amino acid substitutions is related to the biotechnological application of the studied reaction for protein purification.[16] D-Amino acids, which are present, e.g., in natural and semisynthetic antibiotics, provide them with slower rates of degradation, compared to corresponding L-isomers, thanks to a better resistance to enzymatic hydrolysis.[17,18]

We followed the effects of our substitution strategy by hydrolysis rate measurements using HPLC, complemented by a spectroscopic (UV−vis and circular dichroism) and potentiometric characterization of hydrolytic complexes. The reaction mechanism presented in Scheme 1 indicates that the N-terminal leaving group does not participate in the reaction directly. In order to verify this point, we also synthesized and studied the hydrolysis of a parallel series of peptides containing

Received: October 16, 2012
Published: February 21, 2013

   dx.doi.org/10.1021/ic3022672 | *Inorg. Chem.* 2013, 52, 2422−2431

Scheme 1. Molecular Mechanism of Ni(II)-Dependent Peptide Hydrolysis of the Ala-Ser Bond in Ac-GASRHWKFL-NH_2 Peptide Sequence[14,a]

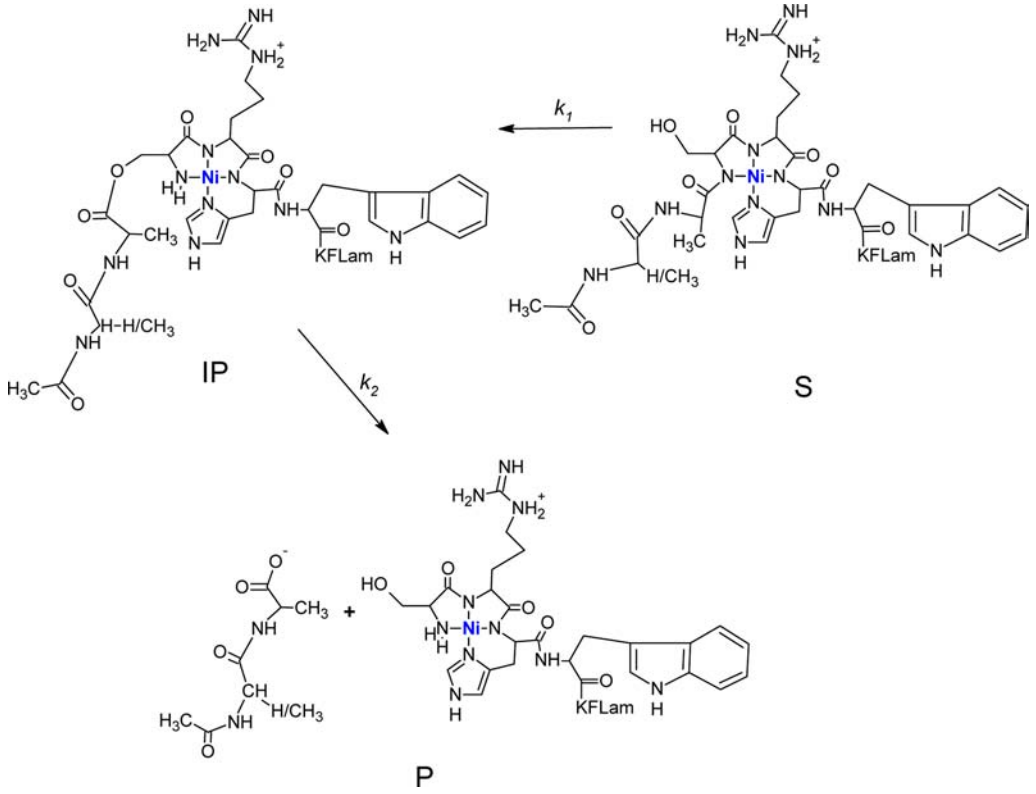

[a]S, substrate; IP, intermediate product (ester); P, final reaction products; k_1 and k_2, pseudo-first order rate constants for the formation of IP and P, respectively.

reversed N-terminal dipeptides, the standard Ac-GA, and the Ac-AG.

Molecular modeling studies were carried out to clarify the relationship between orientation of the side chains in the hydrolytic complex and experimentally determined rates of peptide bond hydrolysis reactions. Simulated annealing was performed to find the lowest energy conformers of Ni(II)-peptide complexes.

EXPERIMENTAL SECTION

Materials. *N*-α-9-Fluorenylmethyloxycarbonyl (F-moc) amino acids were purchased from Sigma-Aldrich and Fluka Co. Trifluoroacetic acid (TFA), piperidine, *N*-hydroxybenzotriazole (HOBt), *N*-[(1*H*-benzotriazol-1-yl)(dimethylamino) methylene]-*N*-methylmethanaminiumtetrafluoroborate *N*-oxide (TBTU), chloranil, triisopropylsilane (TIS), *N*,*N*-diisopropylethylamine (DIEA), and nickel(II) chloride hexahydrate were obtained from Sigma-Aldrich. TentaGel S RAM resin was obtained from Rapp Polymer Inc. Acetonitrile (HPLC grade) was obtained from Rathburn Chemicals Ltd. Pure sodium hydroxide was obtained from Chempur. HEPES (≥99.5%) was purchased from Carl Roth GmbH.

Peptide Synthesis. Peptides were synthesized in the solid phase according to the F-moc protocol.[19] The peptides AGdW and AGdK (see Table 1 for abbreviated names of individual peptides) were synthesized manually, while all others were synthesized using an automatic synthesizer (Protein Technology Prelude). Each coupling and deprotection step was verified using chloranil test, with 2% p-chloranil in DMF (w/v) plus 2% acetaldehyde in DMF (v/v).[19] All syntheses were accomplished on a TentaGel S RAM resin using HOBT in the automatic synthesis and TBTU in the manual synthesis as coupling reagents, both in the presence of DIEA. In all cases the cleavage was done manually by a reagent composed of 95% TFA, 2.5% TIS, and 2.5% water. The acetylation of the N-terminus was carried out in 20% acetic anhydride in DCM in the presence of pyridine. The peptides were purified by HPLC (Breeze, Waters) using an analytical C18 column (ACE 250 × 4.6 mm^2) monitored at 220 and 280 nm. The eluting solvent A was 0.1% (v/v) TFA in water, and solvent B was 0.1% (v/v) TFA in 90% (v/v) acetonitrile. The substrate and products were separated in the linear gradient of 20−40% B over 20 min,

Table 1. Peptides Synthesized for this Study[a]

peptide name	sequence
GA Family	
GA-all-L	Ac-GASRHWKFL-am
GAdS	Ac-GAsRHWKFL-am
GAdR	Ac-GASrHWKFL-am
GAdH	Ac-GASRhWKFL-am
GAdW	Ac-GASRHwKFL-am
GAdK	Ac-GASRHWkFL-am
GAdSdW	Ac-GAsRHwKFL-am
GAdSdR	Ac-GAsrHWKFL-am
GAdSdH	Ac-GAsRhWKFL-am
GAdRdH	Ac-GASrhWKFL-am
GA5d	Ac-GAsrhwkFL-am
AG Family	
AG-all-L	Ac-AGSRHWKFL-am
AGdS	Ac-AGsRHWKFL-am
AGdR	Ac-AGSrHWKFL-am
AGdH	Ac-AGSRhWKFL-am
AGdW	Ac-AGSRHwKFL-am
AGdK	Ac-AGSRHWkFL-am

[a]D-Amino acids are labeled with small letters.

dx.doi.org/10.1021/ic3022672 | Inorg. Chem. 2013, 52, 2422−2431

followed by 7 min of isocratic elution at 100% B, at the flow rate of 1 mL/min. The correctness of molecular masses of peptides was confirmed using a Q-Tof1 ESI-MS spectrometer (Waters). In all peptides the N and C termini were blocked by acetylation and amidation, respectively. Figure S1 shows the mass spectra for substrate and C-terminal hydrolysis product of GAdK as an example.

HPLC Measurements of Hydrolysis Rates. The hydrolysis tests were performed in 20 mM of HEPES at pH 8.2 and the temperature of 30 °C (unless indicated otherwise) in a thermoblock (J.W. Electronics), controlled within ±0.2 °C. This temperature was chosen on the basis of previous studies to optimize the data collection timing. The samples contained 1 mM peptide and 1.25 mM Ni(II), to maintain correspondence with previous mechanistic studies.[13,14] The aliquots were collected typically at 0, 15, 30, 45, 60, 90, 120, 180, 240, 300, 360, and 480 min. For slow reactions the aliquots were also collected daily up to five days. Controls containing peptide and buffer, but not Ni(II), were gathered at the same time points. The 50 μL aliquots were added to 50 μL of 1% (v/v) TFA to stop the reaction, and the final acidified solutions were stored at 4 °C. For analysis, reaction mixtures were diluted by water (20 μL of water to 40 μL of solution) in inserts and placed in the autosampler carousel. A 10 μL portion of each sample was injected into the HPLC system (Empower, Waters), equipped with an analytical C18 column. The eluting solvent A was 0.1% (v/v) TFA in water, and solvent B was 0.1% (v/v) TFA in 90% (v/v) acetonitrile. The chromatograms were obtained at 220 and 280 nm. The relative amounts of product (P), intermediate product (IP), and substrate (S) in each chromatogram were calculated by peak integration using Origin 8.1.

In addition to the aforementioned HEPES protocol which was used for all peptides, the hydrolysis of GA-all-L was measured in Tris buffer, under analogous conditions, and also at pH 9.5 at 0 °C (ice bath). Also during CD kinetic studies (see below), the aliquots withdrawn from reaction mixtures immediately prior to recording the spectra were analyzed by HPLC using the protocol described above.

Circular Dichroism. CD spectra were recorded in the range 300−800 nm, on the Jasco 815 spectropolarimeter. The samples contained 0.33 mM peptide in PTB buffer (40 mM phosphate, 20 mM Tris, and 20 mM borax, pH 9.5) alone or with 0.3 mM Ni(II). The peptides of the GA family were studied. The Ni(II) complexes were first measured at 5 °C, then the temperature was increased, and the hydrolysis was followed by periodic recording of the spectra, typically within 8 h. For slow reactions the aliquots were also collected daily up to five days. The increased temperature was adjusted to individual peptides, as follows: the GA-all-L peptide was studied at 20 and 30 °C. For GAdH and GAdR analogues the temperature was increased to 45 °C. For the GA-all-L, GAdK, and GAdW, the final temperature was 20 °C due to a comparatively fast hydrolysis process. For GAdS, the incubation started from 5 °C, and the temperature was increased successively to 15, 30, and 50 °C and then decreased sequentially to 30, 15, and 5 °C.

UV−Vis Spectroscopy. UV−vis spectra were recorded in the range 300−800 nm, on a Cary 50-Bio (Varian) UV−vis spectrometer. The solution contained 1.0 mM peptide and 0.9 mM Ni(II). The peptides were dissolved in 4 mM HNO_3, containing 96 mM KNO_3. The pH of the solution was adjusted manually in the range 2−12, by adding small amounts of concentrated NaOH.

Potentiometry. Potentiometric titrations of GA-all-L, GAdS, GAdH, and GAdSdH peptides were performed on a Metrohm automatic titrator, using InLab 422 combined glass-Ag/AgCl electrode (Metrohm), calibrated daily by nitric acid titrations.[20] The 0.1 M NaOH (carbon dioxide free) was used as titrant. Sample volumes of 1.5−2 mL were used. The samples contained 1 mM peptides, dissolved in 4 mM HNO_3 containing 96 mM KNO_3. The Ni(II) complex formation was studied using a 5−10% excess of peptides over added $NiCl_2$. The pH range for all potentiometric experiments was from 2.7 to 11.6. All experiments were performed under argon at 25 °C. The data were analyzed using the SUPERQUAD program.[21] Additional calculations were performed using the HYPERQUAD suite.[22] There were 3−5 titrations included simultaneously into calculations, separately for protonation and Ni(II) complexation.

Kinetic Analysis. The calculations of reaction rates depended on the presence of the intermediate reaction product (IP). For the reactions where IP was detected, the set of three equations (Kinet A, Kinet B, and Kinet C) was used to obtain the rate constants k_1 and k_2 (see Scheme 1). For reactions without detectable IP, Kinet A was used to find the substrate decay rate constant. As a double check in these cases, the product formation constant, in principle identical to k_1, was fitted using Kinet D.

Kinet A:

$$y = A_0 \times \exp(-k_1 \times x)$$

Kinet B:

$$y = \left(\frac{k_1 \times A_0}{k_2 - k_1}\right) \times (\exp(-k_1 \times x) - \exp(-k_2 \times x))$$

Kinet C:

$$y = A_0 \times \left(1 + \left(\frac{1}{k_1 - k_2}\right)\right) \times (k_2 \exp(-k_1 \times x) - \exp(k_2 \times x)))$$

Kinet D:

$$y = A_0 \times (1 - \exp(-k_2 \times (x)))$$

In these equations y is a molar fraction of a given species, x is the time axis, and A_0 denotes the initial concentration of the substrate.

Molecular Mechanics Calculations. Molecular mechanics calculations for Ni(II)−peptide complexes were carried out with the aid of YASARA software[23] with the AMBER03 forcefield.[24] During the simulation the square planar arrangement of donor atoms around the Ni(II) ion was maintained using improper dihedral restraints. Simulated annealing was performed in 1000 cycles, consisting of 9 ps heating from 300 to 1100 K and then 4.512 ps cooling to 300 K, 4.5 ps equilibration period at 300 K, followed by energy minimization. The script for calculations was built by us on the basis of available scripts for NMR structure refinement in vacuum in YASARA package. The change introduced was using more steps for gradual increment of nonbonding forces during the cooling phase. The resulting structures were clustered according to the conformation of His Cβ in the 6-membered chelate ring. Lowest energy conformers were used as a representation of the structure of the complex. Molecular graphics were created with YASARA[23] and POVRay.[25]

The AMBER03 forcefield does not contain topologies for square planar geometry around the Ni(II) ion. Therefore, new topologies were created for Ni(II) and for residues coordinated by this ion: Ser, Arg, and His. Bond lengths and angles were taken from the structure of a highly analogous complex of Ni(II) with glycylglycyl-α-hydroxy-D, L-histamine.[26] Point charges were calculated using the MOPAC2009 software[27] with the semiempirical PM6 method.[28] These calculations were carried out for the structure of complex of Ni(II) with the model peptide Ser-Arg-His with acetyl and N-methyl groups on the termini, to mimic respective peptide bonds. The initial structure was obtained on the basis of the previously modeled complex,[13] modified by using the combination of YASARA and MOPAC2009 software. The surplus charges from capping groups was distributed on main chain atoms (Cα, Cβ, C, O, N, Hα) to make the Ni(II) complex with the Ser-Arg-His fragment neutral. Script for optimization of geometry of the Ni(II)-[Ac-SRH-NMe] complex in MOPAC2009 and partial charges of SRH residues and Ni(II) in the square planar complex, calculated by MOPAC2009, are given in Supporting Information Tables S1 and S2, respectively.

RESULTS

HPLC Studies of Reaction Rates. The analysis of hydrolysis reaction was performed by HPLC, according to the methodology established previously.[13,14] The assignment of

dx.doi.org/10.1021/ic3022672 | Inorg. Chem. 2013, 52, 2422−2431

individual peaks was done by comparison with control experiments in the absence of Ni(II) ions (substrate S vs intermediate product IP, both having the same molecular mass, but differing by retention times) and by mass spectrometry (C-terminal reaction product P). Figure 1 presents examples of

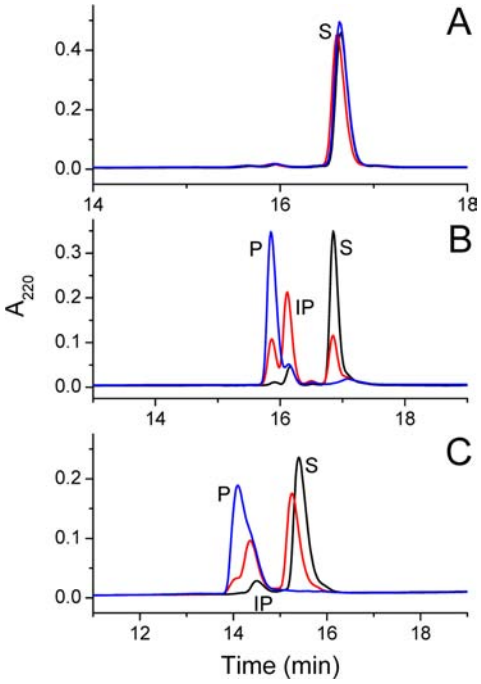

Figure 1. HPLC chromatograms of GAdS (A), GA-all-L (B), and GA5d (C), all 1 mM, incubated at 30 °C with 1.25 mM Ni(II) ions in 20 mM HEPES, pH 8.2. S, substrate; IP, intermediate product, P, product. Incubation times of 0 (black), 90 (red), and 480 (blue) min are shown.

chromatograms, which illustrate the separation and identification of reaction substrate and products. Our previous work indicated HEPES as the most suitable buffer for Ni(II) hydrolysis experiments.[14] The hydrolysis in Tris was slower than in HEPES, apparently due to its weak ability to compete for Ni(II) ions. We decided to compare the rates of hydrolysis in HEPES and Tris again for the GA-all-L peptide, because our current experiments were performed at a different (lower) temperature, and because previously we calculated rate constants in a different fashion, by adding the intermediate product into the substrate or the product instead of treating it explicitly. The first reaction step, described by first order rate constant k_1 in Scheme 1, was significantly faster in HEPES than in Tris ($23.5 \pm 0.9 \times 10^{-5}$ s^{-1} vs $15.7 \pm 0.5 \times 10^{-5}$ s^{-1}), while the rates for the second step, described by k_2, were nearly the same for both buffers ($10.2 \pm 0.3 \times 10^{-5}$ s^{-1} vs $11.5 \pm 0.3 \times 10^{-5}$ s^{-1}) (see Figure 2). All subsequent studies were therefore performed in HEPES, as a noninterfering medium.

Table 2 presents the hydrolysis reaction rates for all peptides studied in 20 mM HEPES at 30 °C and pH 8.2. These included the template all-L peptides (GA-all-L and AG-all-L) and their single D-amino acid substitutions in all five positions considered relevant to the molecular mechanism of hydrolysis: Ser, Arg, His, Trp, and Lys. The GA family also included double substitutions at S/H, S/R, S/W, and H/R positions, and the peptide contained D-analogues at all five positions listed.

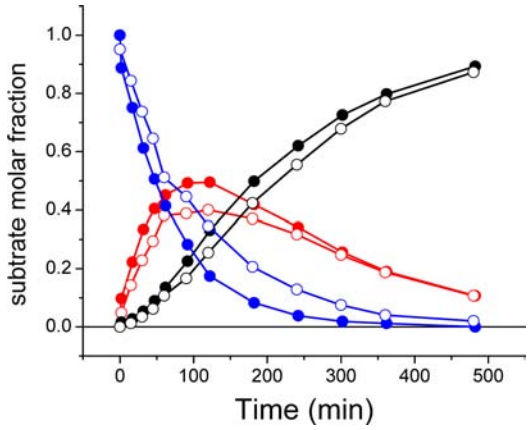

Figure 2. Comparison of hydrolysis of 1 mM GA-all-L in the presence of 1.25 mM Ni(II) in 20 mM HEPES (●), and 20 mM Tris (○). The formation of reaction substrate (blue), intermediate product (red), and product (black) is shown.

The effects of single substitutions were the same in both families of peptides. The unsubstituted analogues were hydrolyzed at the fastest pace, followed by slightly less active D-Lys and D-Trp. The hydrolysis was significantly slower for D-Arg and yet slower for D-His. The D-Ser analogues were completely inactive. Among double substitutions, GAdSdW was also inactive, but the GAdSdR peptide was hydrolyzed, albeit very slowly, with the rate very similar to that of GAdH (Figure 3). Likewise, the GAdSdH peptide was hydrolyzed with a rate similar to the GAdR analogue. GAdRdH was completely resistant to hydrolysis, like GAdS. However, the switch of all five residues from L to D, in the GA5d analogue, restored the susceptibility to hydrolysis to values comparable with those of the GA-all-L.

In order to confirm the absence of hydrolysis in the D-Ser analogues, the hydrolysis of four peptides was also studied at pH 11.6, where the rate of hydrolysis is maximal, due to the 100% abundance of the hydrolytic complex.[14] These results are shown in the last column of Table 2. At this pH the reaction is characterized solely with k_1, which describes the substrate decay and the final product formation. This is due to a very low stability of the intermediate ester at elevated pH. These data confirmed the absence of reactivity of GAdS. Also, the rates in complementarily substituted GAdR and GAdSdH were practically identical.

Coordination Studies. To gain better insight into the reason of inactivity of D-Ser analogues, we selected four peptides, the fast-reacting GA-all-L, the slow reacting GAdH, the inactive GAdS, and the double substituted GAdSdH, to study their Ni(II) binding properties. We determined stability constants of the respective Ni(II) complexes by potentiometry, and confirmed the complex formation by UV−vis spectroscopy (see Figure S2 for an example). Table 3 presents the binding constants, which are illustrated by species distribution plots, with overlaid intensities of d−d bands of low spin Ni(II) complexes (Figure 4). Table 4 provides the parameters of d−d bands of these complexes. The D-Ser analogues exhibited spectra of typical square planar complexes with only subtle changes compared to L-analogues. Also, stabilities of complexes demonstrated that L to D substitutions had little effect on Ni(II) coordination geometry and binding constants.

Circular Dichroism Spectroscopy. Having established that differences in hydrolytic reactivity are not due to

dx.doi.org/10.1021/ic3022672 | Inorg. Chem. 2013, 52, 2422−2431

Table 2. First Order Rate Constants ($s^{-1} \times 10^{-5}$) Determined for Ni(II)-Dependent Hydrolysis of Peptides at 30 °C and pH 8.2 (20 mM HEPES)[a]

	pH 8.2 (20 mM HEPES)					pH 11.6 (PBT buffer)
GA family	$k_1 \pm$ SD	$k_2 \pm$ SD	AG family	$k_1 \pm$ SD	$k_2 \pm$ SD	$k_1 \pm$ SD
GA-all-L	23.5 ± 0.9	10.2 ± 0.3	AG-all-L	112 ± 10	9.8 ± 0.5	99 ± 11
GAdK	19.3 ± 0.6	5.5 ± 0.2	AGdK	42.3 ± 0.6	6.2 ± 0.09	
GAdW	7.4 ± 0.1	6.2 ± 0.1	AGdW	10.2 ± 0.1	4.8 ± 0.8	
GAdR	1.6 ± 0.05	4.09 ± 0.3	AGdR	7.5 ± 0.2	6.9 ± 0.2	3.2 ± 0.7
GAdH	0.1 ± 0.01	7 ± 1.9	AGdH	1.5 ± 0.05	5.5 ± 0.4	
GAdS	n.d.	n.d.	AGdS	n.d.	n.d.	n.d.
GA5d	22.4 ± 0.5	4.4 ± 0.07				
GAdSdH	1.9 ± 0.05	2.0 ± 0.1				3.08 ± 0.04
GAdSdR	0.13 ± 0.03	n.d.				
GAdSdW	n.d.	n.d.				
GAdRdH	n.d.	n.d.				

[a]The last column shows rate constants for four selected peptides at 30 °C and pH 11.6 (PBT buffer). n.d.: hydrolysis not detected.

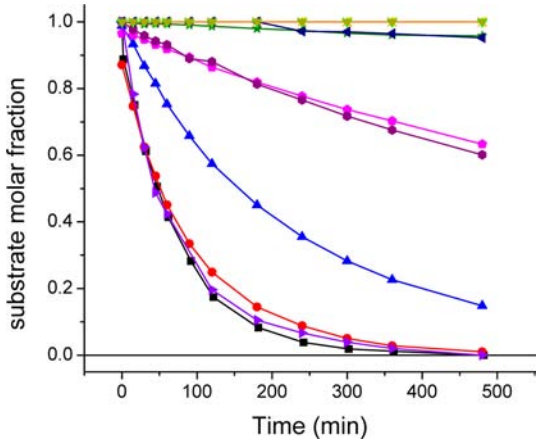

Figure 3. Substrate decay curves for GA family peptides: GA-all-L (black), GAdK (red), GAdW (blue), GAdR (magenta), GAdH (olive), GAdS (yellow), GAdSdH (purple), GAdSdR (navy), GAdSdW (green), GAdRdH (orange), and GA5d (violet). The reactions were carried out at pH 8.2 in 20 mM HEPES buffer, and concentrations of peptides and Ni(II) were 1.0 mM and 1.25 mM, respectively. The traces for GAdS, GAdSdW, and GAdRdH overlap completely (no reaction).

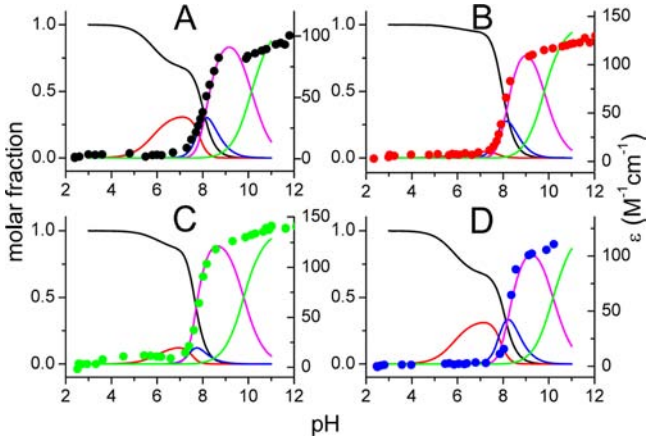

Figure 4. Species distribution plots calculated for 1 mM of Ni(II) and 1 mM of four peptides: (A) GA-all-L, (B) GAdH, (C) GAdS, and (D) GAdSdH. Individual species are marked as follows: Ni^{2+}, black, 1N, red; 3N, blue; 4N, magenta and green (differing by deprotonation of the noncoordinating Lys side chain). 1N, 3N, and 4N denote the number of nitrogen atoms coordinated to Ni(II). Intensities of d−d bands of low spin Ni(II) complexes are overlaid (●).

differences in Ni(II) complex formation, we resorted to CD spectroscopy as a sensitive tool for studying stereochemistry. Figure 5 presents the visible range CD spectra of Ni(II) complexes of GA family peptides. These spectra were recorded at pH 9.5 to ensure full formation of complexes (cf. Figure 4), and at 5 °C in order to eliminate the interference from hydrolysis during the collection of the spectra. The spectra exhibit a huge variability of d−d band patterns, but in all cases the energies of transitions were similar and consistent with square-planar geometry. The parameters of these spectra are provided in Table 4.

Four pairs of peptides exhibited spectra being near mirror images of each other. These are shown in Figure S3. These mirror image pairs are related to substitutions within the Ser-Arg-His sequence.

We then followed hydrolysis of GA family peptides by CD. These experiments were aimed at establishing the conformational consequences of the cleavage of the Ala-Ser bond. The progress of reaction was controlled independently by

Table 3. Logarithmic Protonation and Ni(II) Complex Formation Constants of Peptides Determined at 25 °C and I = 0.1 M (KNO_3)[a]

peptide	NiHL	NiL	$NiH_{-1}L$	$NiH_{-2}L$	$NiH_{-3}L$	HL	H_2L
GA-all-L	12.93(2)	n.d.[b]	−2.62(1)	−10.694(8)	−20.98(1)	10.23(4)	16.56(2)
GAdS	12.32(6)	n.d.	−2.52(3)	−9.67(1)	−19.47(1)	10.17(3)	16.91(4)
GAdH	11.7(2)	n.d.	−2.99(2)	−11.02(1)	−20.83(1)	9.6(1)	16.5(2)
GAdSdH	13.15(2)	n.d.	−2.6(2)	−10.90(1)	−21.16(3)	10.13(2)	16.46(4)

[a]Numbers in parentheses denote standard deviations on the last digits. Standard deviations on the least significant digits, provided by SUPERQUAD or HYPERQUAD, are given in parentheses.[21,22] [b]n.d., not detected.

dx.doi.org/10.1021/ic3022672 | Inorg. Chem. 2013, 52, 2422−2431

Table 4. Parameters of d−d Bands of Absorption and CD Spectra of NiH$_{-2}$L Complexes of GA Family Members[a]

peptide	λ	$\Delta\varepsilon$	λ	$\Delta\varepsilon$	λ	$\Delta\varepsilon$	λ_{max}	ε
GA-all-L	503	−0.69			446	0.49	424	103
GAdK	501	−1.13			443	0.79		
GAdW	495	−1.40			437	0.83		
GAdR			469	1.08				
GAdH	503	0.25			417	−2.49	432	145
GAdS	495	−1.50			416	2.43	430	155
GAdSdR	518	−0.39			420	3.28		
GAdSdH			464	−1.22			442	199
GAdRdH	490	1.55			413	−2.73		
GA5d	504	1.10			440	−0.45		

[a]Units for λ and λ_{max} are nm, for ε and $\Delta\varepsilon$ are M^{-1} cm^{-1}.

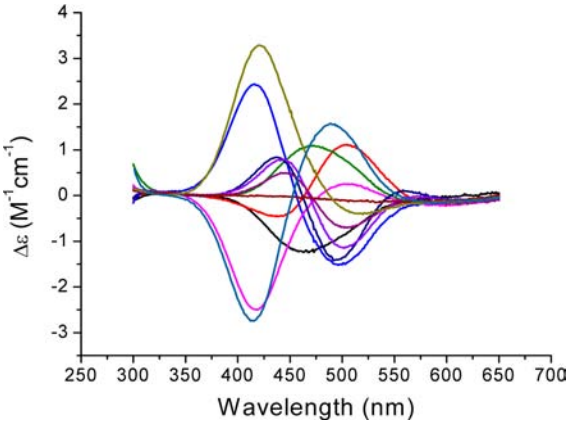

Figure 5. The d−d range CD spectra of Ni(II) complexes of GA family peptides in PTB buffer, pH 9.5, recorded at 5 °C. Peptides and Ni(II) concentrations were 0.33 mM and 0.3 mM, respectively. GA-all-L, purple; GAdK, violet; GAdS, blue; GAdR, olive; GAdW, navy; GA5d, red; GAdSdH, black; GAdSdR, dark yellow; GAdH, pink; GAdRdH, dark blue; baseline (peptides alone), wine.

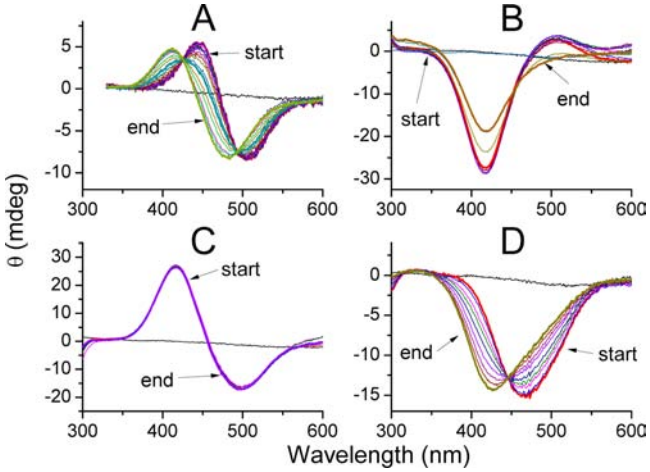

Figure 6. CD monitored incubation of GA-all-L (A), GAdH (B), GAdS (C), and GAdSdH (D) in PTB buffer, pH 9.5. Peptides and Ni(II) concentrations were 0.33 and 0.3 mM, respectively. The first and last recorded spectra are marked with start and end labels, respectively. Variable incubation temperatures are provided in the Experimental Section.

submitting the aliquots collected from the samples immediately before recording the spectra to HPLC analysis. Supporting Information Figure S4 illustrates the equivalence of both methods of monitoring the reaction progress, using the GA-all-L peptide as an example. Figure 6 presents several examples of CD-monitored hydrolysis reactions. The remaining results are shown in Figure S5. The susceptibility to hydrolysis seen by CD spectroscopy agreed with results of HPLC studies for all cases (Table S3). In terms of CD spectral changes, the blue shift of the spectral bands was seen commonly, but the overall spectral patterns were largely conserved. The spectra of complexes of two peptides subjected to this assay which were resistant to hydrolysis in HPLC tests, GAdS (Figure 6C) and GAdRdH (Figure S5D), remained unchanged, even at elevated temperatures.

The comparison of HPLC and CD data enabled calculation of the CD spectra of Ni(II) complexes with reaction products. These spectra are shown in Figure S6.

The mirror image pattern resulting from single or double substitutions within the three amino acid residues forming bonds with the Ni(II) ion encouraged us to check whether the contributions of individual residues to the spectra may be additive, as stipulated by the hexadecant rule.[29,30] Assuming that the contributions of enantiomers differ only by the sign, for instance D-Ser = negative of L-Ser, we were able to confirm this additivity, as shown for two examples in Figure 7. Respective calculations are provided in the Table S4.

Molecular Modeling. In our previous study the spatial relationships between side chains of the residues forming the hydrolytic complex were established.[13] The bulky side chain of the residue placed between Ser and His (X in the library notation) created the molecular crowding near the Ser residue, while the bulky side chain of the residue following His (Z in the library notation) acted likewise on the other side of the chelate plane. To simplify description, we will call the positions of side chains of L-Ser and L-Arg as "above".

Our more detailed calculations presented here confirmed the previously noted fact that the 6-membered chelate ring, formed as a result of coordination of bidentate His coordination to Ni(II), can adopt two conformations, differing in the puckering of Cβ.[31] Figure 8 illustrates this phenomenon for GA-all-L. It is striking that the conformation of the 6-membered ring determines the localization of N-terminal residues, GA. The bending of the peptide backbone by the coordinated Ni(II) ion brings the His side chain close to these N-terminal residues, thus contributing to steric hindrance. The Ni(II) ion and nitrogen donors are not coplanar anymore, as it was observed for Ni(II) complex with glycylglycyl-α-hydroxy-D, L-histamine[26] with N-terminal amino group. The position of alanine side chain in the modeled structures is fixed and oriented away from

dx.doi.org/10.1021/ic3022672 | Inorg. Chem. 2013, 52, 2422−2431

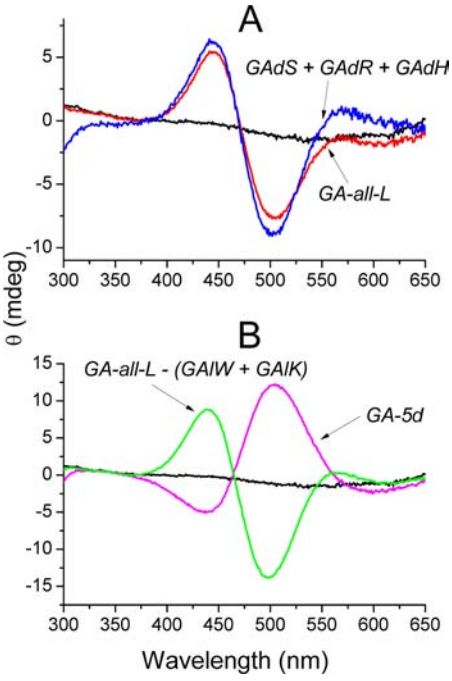

Figure 7. Examples of spectral arithmetics, reproducing identical or mirror image patterns of d−d bands of Ni(II) complexes on the basis of the additivity of contributions of individual amino acid residues: (A) GA-all-L = GAdS + GAdR + GAdH; (B) GA-all-L - (GAlW+ GAlK) is nearly a mirror image of GA-5d (see Table S4 for the details of calculations).

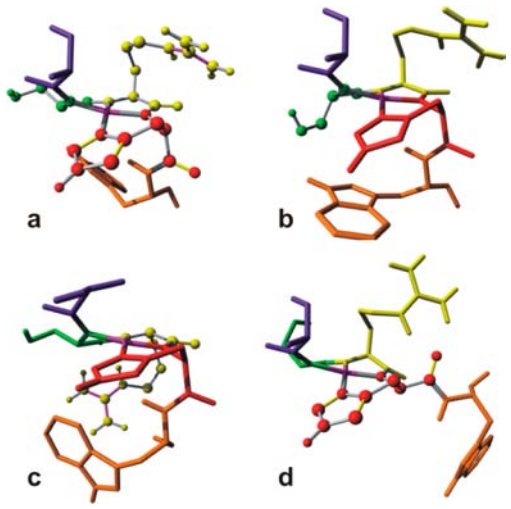

Figure 8. Modeled structures of complexes: (a) Ni(II)-GA-all-L, (b) Ni(II)-GAdS, (c) Ni(II)-GAdR, (d) Ni(II)-GAdH. Panels represents lowest energy structures of the same conformer of ring puckering of the Cβ of the His residue (it does not necessarily mean the global minimum). The coloring scheme is as follows: Ala, purple; Ser, green; Arg, yellow; His, red; Trp, orange; Ni(II), magenta. Part of the peptide, consisting of Ac-Gly- on N-terminus and -Lys-Phe-Leu-NH_2 on C-terminus, and aliphatic hydrogens were omitted for clarity. The ball and stick representation is used to mark L-Ser, L-Arg, L-His (a) and D-analogs (b−d). Structures are superposed on atoms of Ni(II), Ser, Arg, and His residues.

arginine side-chain, but close to the oxygen of cleaved peptide bond.

Kinetic studies revealed that the substitution to D-amino acid of the five residues relevant to hydrolysis, SRHWK, restores the peptide hydrolysis rate of the GA-all-L analogue. Moreover, the CD spectrum of this GA5d peptide is nearly a mirror image of the initial one. Thus, it is not surprising that structures of GA5d obtained from molecular mechanics calculations are mirror images of GA-all-L (Figure 9). Not only are the Ser, Arg, and

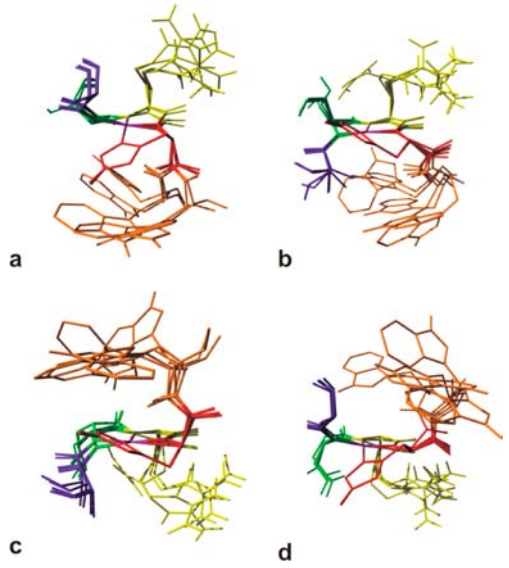

Figure 9. Modeled structures of Ni(II)-GA-all-L complex (a, b) are nearly mirror images of those of Ni(II)-GA5d complex (c, d). Panels represent five lowest energy structures of each possible ring puckering of the Cβ of the His residue. The coloring scheme is as follows: Ala, purple; Ser, green; Arg, yellow; His, red; Trp, orange; Ni(II), magenta. Part of the peptide, consisting of Ac-Gly- at the N-terminus and -Lys-Phe-Leu-NH_2 at the C-terminus, and aliphatic hydrogens were omitted for clarity. Structures are superposed on atoms of Ni(II) and Ser, Arg, and His residues.

Trp side chains moved to the opposite side of the coordination plane, but also there is a switch in the ring puckering at His Cβ. Consequently, the N-terminal residues are moved to the opposite side of the chelation ring, restoring the spatial relations between side chains in the Ni(II)-GA5d complex to the GA-all-L situation.

DISCUSSION

We started our study verifying the buffer effect on the rate of hydrolysis of the GA-all-L peptide at pH 8.2. As we found, the difference between HEPES and Tris was limited to the first reaction step, significantly faster in HEPES. This effect is consistent with the higher abundance of the active complex in noncoordinating HEPES,[32] relative to the Tris solution, where Ni(II)-Tris complexes are formed (at 25 °C and I = 0.10 M K_a = $10^{2.74}$ M^{-1}) which compete for Ni(II) with the peptide.[33] The similarity of rates for the ester hydrolysis between the two buffers is consistent with the solvent-only dependent hydrolysis of the ester bond (Scheme 1, step 2).

The hydrolysis rate constants presented in Table 2 were determined at pH 8.2 and pH 11.6. The lower of these pH values was chosen in our previous studies as a way to select the fastest reacting peptides. At these conditions the observed k_1 is the combination of the maximum (intrinsic) rate of the acyl shift process for the given active complex and the abundance of this complex. These data revealed several interesting systematic effects.

dx.doi.org/10.1021/ic3022672 | Inorg. Chem. 2013, 52, 2422−2431

First, there was no reaction for peptides containing the individual D-Ser or the double D-Ser + D-Trp substitutions. However, the reactivity, although much slower, compared to the reference all-L peptides, was restored in D-Ser + D-Arg and D-Ser + D-His peptides. On the other hand, the D-Arg + D-His substitution resulted in no reaction, like D-Ser. Single substitutions D-Arg and D-His, while slowing the reaction down, did not disable it completely. The complementarity of L/D substitutions within the SRH triad is quantitative; that is, the L/D substitution of one of these three amino acids gives the same effect as the double substitution of the other two (Table 5). On the other hand, the effects of D-Trp and D-Lys substitutions were much smaller. This is particularly striking for Trp. This residue does not participate in Ni(II) coordination, but has a very significant effect on the hydrolysis rate, compared to less bulky residues.[13,14] The substitution of all five residues to D-analogues reproduced the reaction rates of the all-L peptide. The order of rate constants was preserved for all single substitutions we introduced to the peptides of the AG series, although the k_1 hydrolysis rates were systematically higher. There was no systematic effect of these substitutions on k_2, and all values remained within a relatively narrow range.

Table 5. Summary of Activities for the Ser-Arg-His Part of the Sequence[a]

	rate constant							
AA	*23*	**0**	***1.6***	0.1	0.1	***1.9***	**0**	*22*
S	*L*	**D**	***L***	L	D	***D***	**L**	*D*
R	*L*	**L**	***D***	L	D	***L***	**D**	*D*
H	*L*	**L**	***L***	D	L	***D***	**D**	*D*
activity	+	−	+	+	+	+	−	+

[a]Peptides with similar rate constants have mirror image in CD spectra. GA-all-L and GA5d have high rate constants (italic type). GAdS and GAdRdH are inactive (bold type), GAdR and GAdSdH are similar in activity (bold italic type), and GAdH and GAdSdR are very weak but still active (regular type). Columns with the same type style mark peptides with the same reactivity, but mirror image CD spectra.

The absence of hydrolysis for the GAdS peptide and the equivalence of GAdSdH and GAdR substitutions were also confirmed by the measurement of the hydrolysis rate at pH 11.6. At this pH the ester hydrolysis is immediate, and therefore, the intermediate product is not detected. The observed rate is maximal, because the abundance of the active complex is 100%. Therefore, shifting the Arg residue to the opposite chirality slows the reaction down by a factor of 30, compared to the GA-all-L peptide.

The Ni(II) complex formation of the same four peptides was studied by potentiometry (Table 3) and spectroscopy. Figure 4 compares the potentiometry-based complex species distribution with UV−vis spectral parameters characteristic for square planar complex, positively verifying the correctness of the potentiometric data analysis. These data demonstrate that there are no significant differences between the four studied peptides with respect to the 4N complex formation.

All these observations can be collectively summarized as follows. The k_1 rate constant is strongly dependent on the relative position of Ser versus Arg and His, and the reaction is abolished when the Ser residue has the opposite chirality to both Arg and His. The small effect of changing the chirality of Trp and Lys is consistent with the postulated role of the C-terminal residues, beyond the Ni(II)-binding His as providing general steric hindrance, rather than specific interactions (see Scheme 1). The quantitative, but not qualitative, effect of changing the N-terminal dipeptide sequence is also consistent with the effect of these flanking sequences as limiting the conformational space available to Ser side chain, the acceptor of the acyl group. The latter is confined in space by Ni(II) coordination to the nitrogen of the breaking peptide bond. This point is further confirmed by the fact that the symmetry of d−d CD spectra of hydrolysis substrates and products is the same (Figures 6 and S5). Therefore, the stereochemistry of the reaction site is fundamentally controlled by interactions between the Ni(II) bound Ser, Arg, and His residues.

The molecular mechanics calculations performed previously for the GA-all-L peptide showed that the Trp residue adopts the position "below" the chelate plane, which leads to the enhancement of the reaction rate.[13] The results of calculations for complexes of GA-all-L, GAdS, GAdR, and GAdH, presented in Figure 8, show that the reversal of the chirality of Ser and Arg directs their side chains below the coordination plane. In the case of His, the D-amino acid substitution does not affect the position of its side chain, because it is bound by Ni(II). However, regarding the side chain of the next residue, Trp is moved from "below" the coordination plane to "above" it.

Our previous studies of peptide libraries demonstrated a need for a bulky residue "below" for effective hydrolysis.[13] The

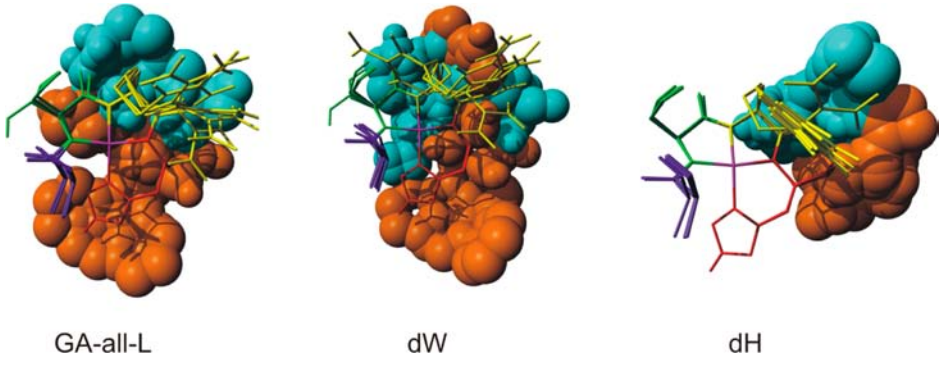

Figure 10. Modeled structures of Ni(II)-peptide complexes. Panels represent view from "above" the coordination plane. The main difference between peptide complexes is in the spatial orientation of tryptophan (orange) and lysine (cyan). Five lowest energy structures of one possible ring puckering of the Cβ of the His residue are superposed on atoms of Ni(II) and Ser, Arg, and His residues. The coloring scheme is as follows: Ala, purple; Ser, green; Arg, yellow; His, red; Trp, orange; Lys, cyan; Ni(II), magenta. Trp and Lys residues are represented as balls. Part of the peptide, consisting of Ac-Gly- on N-terminus and -Lys-Phe-Leu-NH_2 on C-terminus, and aliphatic hydrogens were omitted for clarity.

dx.doi.org/10.1021/ic3022672 | Inorg. Chem. 2013, 52, 2422−2431

library data indicate that the substitution of Trp with Gly, which has no side chain, decreased the reaction rate by more than an order of magnitude. The presence of Trp side chain "above", near the region occupied in D-His peptides by the Ser and Arg side chains, may actually decrease the rate even further by interfering with their roles in the reaction. Therefore, the L- to D-His substitution acts as a Trp (and Lys) switch. The L- to D-Trp substitution has a much lesser effect, because even if tryptophan side chain is moved away, its position can be partially occupied by lysine (Figure 10).

The additivity of contributions of Ser and Arg to the CD pattern indicates that their side chains assume positions in space independently of each other in a "picket fence" fashion we saw in the NMR structure of another square planar Ni(II) complex, VIHN.[34] This explains the additivity of contributions in position X to the reaction rate, which we found in peptide libraries.[13] Altogether, the Ni(II)-assisted peptide bond hydrolysis is only possible when the Ser side chain is confined in space. Our calculations did not pinpoint its exact position relative to the carbonyl moiety of the residue preceding Ser, required for the reaction, but did provide direction for further investigations using structural methods. In this context, it is very interesting to note that all AG family members had higher k_1, but similar k_2 rate constants, compared to their GA peers. According to the absence of significant symmetry changes in CD spectra between the reaction substrates and products, the leaving N-terminal sequence does not affect the geometry of side chains around the Ni(II) ion in the reaction substrate. An interesting possibility to account for these facts is the *cis*−*trans* isomerization of the hydrolyzable peptide bond, proposed very recently to occur in analogous (nonhydrolyzing) Cu(II) peptide complexes.[35] This effect might provide mechanistic explanation for the striking role of residues occupying the space "below" the chelate plane. We are going to investigate this effect of N-terminal sequences in our future work.

Last but not least, our CD spectra demonstrate that the hexadecant rule[29,30] can be extended over Ni(II) complexes including His side chain coordination.

CONCLUSION

The study of effects of D-amino acid substitutions on Ni(II)-assisted peptide bond hydrolysis was originally aimed at improving the rate of reaction. This proved to be impossible, as all stereochemical alterations made around the Ni(II) chelate plane resulted in the decrease of the reaction rate. Instead, we obtained very valuable information about the geometrical requirements of the reaction, which will assist in its further development. We demonstrated that the reaction is only possible when either the side chain of the crucial Ser (or Thr) residue is on the same part of the chelate plane as the next residue in the sequence (Arg), or the side chain of the residue following His (Trp) resides on the opposite side of the plane. The rate of reaction is the fastest when both these conditions are fulfilled. Another novel effect is the strong dependence of the rate of the acyl shift step on the character of the leaving group. Full explanation of these effects will require structural studies of peptides with varied N-terminal sequences. The fact that the reaction is enabled or disabled by stereochemistry of the three Ni(II)-binding amino acid residues paves the way for the full DFT theoretical study of the reaction mechanism, because it determines the minimal sequence which needs to be taken into account in these calculations.

The results of this work, and the aforementioned follow-up studies, will be very useful for screening potential targets of Ni(II) hydrolytic toxicity among human proteins and for designing biotechnological applications of the studied reaction.

ASSOCIATED CONTENT

Supporting Information

Additional figures and tables. This material is available free of charge via the Internet at http://pubs.acs.org.

AUTHOR INFORMATION

Corresponding Author

*E-mail: wbal@ibb.waw.pl. Phone: 48-22-592-2346. Fax: 48-22-658-4636.

Notes

The authors declare no competing financial interest.

ACKNOWLEDGMENTS

This research was supported by the project *Metal-Dependent Peptide Hydrolysis. Tools and Mechanisms for Biotechnology, Toxicology and Supramolecular Chemistry* carried out as part of the Foundation for Polish Science TEAM program, cofinanced from European Regional Development Fund resources within the framework of Operational Program Innovative Economy. The equipment used was sponsored in part by the Centre for Preclinical Research and Technology (CePT), a project cosponsored by European Regional Development Fund and Innovative Economy, The National Cohesion Strategy of Poland.

REFERENCES

(1) International Agency for Research on Cancer. Chromium, Nickel and Welding. *IARC Monographs on the Evaluation of Carcinogenic Risk to Humans*; Lyon, France, Vol. *49*, 1990.
(2) Kurowska, E.; Bal, W. In *Advances in Molecular Toxicology*; Fishbein, J. C., Ed.; Elsevier B.V.: New York, 2010; Vol. *4*, p 85.
(3) Rando, O. J. *Curr. Opin. Genet. Dev.* **2012**, *22*, 148.
(4) Kasprzak, K. S.; Bal, W.; Karaczyn, A. A. *J. Environ. Monit.* **2003**, *5*, 1.
(5) Bal, W.; Jeżowska-Bojczuk, M.; Lukszo, J.; Kasprzak, K. S. *Chem. Res. Toxicol.* **1995**, *8*, 683.
(6) Bal, W.; Lukszo, J.; Kasprzak, K. S. *Chem. Res. Toxicol.* **1996**, *9*, 535.
(7) Bal, W.; Lukszo, J.; Bialkowski, K.; Kasprzak, K. S. *Chem. Res. Toxicol.* **1998**, *11*, 1014.
(8) Bal, W.; Liang, R.; Lukszo, J.; Lee, S. H.; Dizdaroglu, M.; Kasprzak, K. S. *Chem. Res. Toxicol.* **2000**, *13*, 616.
(9) Zoroddu, M. A.; Kowalik-Jankowska, T.; Kozlowski, H.; Molinari, H.; Salnikow, K.; Broday, L.; Costa, M. *Biochim. Biophys. Acta, Gen. Subj.* **2000**, *1475*, 163.
(10) Karavelas, T.; Malandrinos, G.; Hadjiliadis, N.; Mlynarz, P.; Kozlowski, H.; Barsam, M.; Butler, I. *Dalton Trans.* **2008**, 1215.
(11) Nunes, A. M.; Zavitsanos, K.; Del Conte, R.; Malandrinos, G.; Hadjiliadis, N. *Inorg. Chem.* **2010**, *49*, 5658.
(12) Karaczyn, A. A.; Bal, W.; North, S. L.; Bare, R. M.; Hoang, V. M.; Fisher, R. J.; Kasprzak, K. S. *Chem. Res. Toxicol.* **2003**, *16*, 1555.
(13) Krezel, A.; Kopera, E.; Protas, A. M.; Wyslouch-Cieszynska, A.; Poznanski, J.; Bal, W. *J. Am. Chem. Soc.* **2010**, *132*, 3355.
(14) Kopera, E.; Krezel, A.; Protas, A. M.; Belczyk, A.; Bonna, A.; Wyslouch-Cieszynska, A.; Poznanski, J.; Bal, W. *Inorg. Chem.* **2010**, *49*, 6636.
(15) Kurowska, E.; Sasin-Kurowska, J.; Bonna, A.; Grynberg, M.; Poznanski, J.; Knizewski, L.; Ginalski, K.; Bal, W. *Metallomics* **2011**, *3*, 1227.
(16) Kopera, E.; Belczyk, A.; Bal, W. *PLoS ONE* **2012**, *7*, e36350.

(17) Martínez-Rodríguez, S.; Martínez-Gómez, A. I.; Rodríguez-Vico, F.; Clemente-Jiménez, J. M.; Las Heras-Vázquez, F. J. *Chem. Biodiversity* **2010**, *7*, 1531.
(18) Dasgupta, P. *Phamacol.Ther.* **2004**, *102*, 61.
(19) Chan, W.; White, P. *Fmoc Solid Phase Peptide Synthesis: A Practical Approach*; Oxford University Press: Oxford, 2000.
(20) Irving, H.; Miles, M. G.; Pettit, L. D. *Anal. Chim. Acta* **1967**, *38*, 475.
(21) Gans, P.; Sabatini, A.; Vacca, A. *J. Chem. Soc., Dalton Trans.* **1985**, 1195.
(22) Gans, P.; Sabatini, A.; Vacca, A. *Talanta* **1996**, *43*, 1739.
(23) Krieger, E.; Darden, T.; Nabuurs, S.; Finkelstein, A.; Vriend, G. *Proteins* **2004**, *57*, 678.
(24) Duan, Y.; Wu, C.; Chowdhury, S.; Lee, M. C.; Xiong, G.; Zhang, W.; Yang, R.; Cieplak, P.; Luo, R.; Lee, T. A. *J. Comput. Chem.* **2003**, *24*, 1999.
(25) http://www.povray.org/
(26) Bal, W.; Djuran, M. I.; Margerum, D. W.; Gray, E. T.; Mazid, M. A.; Tom, R. T.; Nieboer, E.; Sadler, P. *J. Chem. Soc., Chem. Commun.* **1994**, 1889.
(27) Stewart, J. J. P. *MOPAC2009, Version 11.016W*; Stewart Computational Chemistry, http://OpenMOPAC.net.
(28) Stewart, J. J. P. *J. Mol. Model.* **2007**, *13*, 1173.
(29) Tsangaris, J. M.; Martin, R. B. *J. Am. Chem. Soc.* **1970**, *92*, 4255.
(30) Clayton, R. B.; van Tarnelen, E. E.; Nadeau, R. G. *J. Am. Chem. Soc.* **1967**, *89*, 4661.
(31) Klewpatinond, M.; Viles, J. H. *Biochem. J.* **2007**, *404*, 393.
(32) Sokołowska, M.; Wszelaka-Rylik, M.; Poznański, J.; Bal, W. *J. Inorg. Biochem.* **2009**, *103*, 1005.
(33) Fischer, B.; Haring, U.; Tribolet, R.; Sigel, H. *Eur. J. Biochem.* **1979**, *94*, 523.
(34) Bal, W.; Chmurny, G.; Hilton, B.; Sadler, P.; Tucker, A. *J. Am. Chem. Soc.* **1996**, *118*, 4727.
(35) Cong, X.; Rossetti, G.; Legname, G.; Carloni, P. In *Book of Abstracts;*Copper in Biology, 8th International Copper Meeting; Alghero, Sardinia, Italy, 2012; p 71.

dx.doi.org/10.1021/ic3022672 | *Inorg. Chem.* 2013, 52, 2422−2431